# Enhancement of Parametric Effects in Polariton Waveguides Induced by Dipolar Interactions

D. G. Suárez-Forero,[1,2] F. Riminucci,[2,3] V. Ardizzone,[1,*] N. Karpowicz,[1,†] E. Maggiolini,[1] G. Macorini,[1] G. Lerario,[1] F. Todisco,[1] M. De Giorgi,[1] L. Dominici,[1] D. Ballarini,[1] G. Gigli,[1] A. S. Lanotte,[1,4] K. West,[5] K. Baldwin,[5] L. Pfeiffer,[5] and D. Sanvitto[1,4]

[1]*CNR NANOTEC, Institute of Nanotechnology, Via Monteroni, 73100 Lecce, Italy*
[2]*Dipartimento di Fisica, Università del Salento, Strada Provinciale Lecce-Monteroni, Campus Ecotekne, Lecce 73100, Italy*
[3]*Molecular Foundry, Lawrence Berkeley National Laboratory, One Cyclotron Road, Berkeley, California 94720, USA*
[4]*INFN, Sezione di Lecce, Via per Monteroni, Lecce 73100, Italy*
[5]*PRISM, Princeton Institute for the Science and Technology of Materials, Princeton University, Princeton, New Jersey 08540, USA*

(Received 22 July 2020; accepted 17 February 2021; published 30 March 2021)

Exciton-polaritons are hybrid light-matter excitations arising from the nonperturbative coupling of a photonic mode and an excitonic resonance. Behaving as interacting photons, they show optical third-order nonlinearities providing effects such as optical parametric oscillation or amplification. It has been suggested that polariton-polariton interactions can be greatly enhanced by inducing aligned electric dipoles in their excitonic part. However, direct evidence of a true particle-particle interaction, such as superfluidity or parametric scattering, is still missing. In this Letter, we demonstrate that dipolar interactions can be used to enhance parametric effects such as self-phase modulation in waveguide polaritons. By quantifying these optical nonlinearities, we provide a reliable experimental measurement of the direct dipolar enhancement of polariton-polariton interactions.

DOI: 10.1103/PhysRevLett.126.137401

Adding high nonlinearities to compact, integrated optical circuits could unlock the development of new, fully photonic devices such as ultra-low-power active switches and transistors [1], parametric amplifiers or oscillators and supercontinuum sources [2]. Nonlinearities could even push forward the limit of integrated optics in quantum applications, i.e., universal quantum logic gates [3,4]. Exciton polaritons have demonstrated to be good candidates for supplying nonlinearities to integrated optical platforms. They emerge, in inorganic semiconductors, from the strong coupling between a photonic mode and an electronic excitation (exciton) in quantum wells (QWs). The nonlinearities in such systems, originating from exchange interactions in the excitonic component, have been widely studied in the mesoscopic regime, allowing the demonstration of effects such as optical parametric oscillation, [5], bistability [6], superfluidity [7,8], pattern formation [9] or quantum vorticity [10]. Despite polariton-polariton interactions providing higher nonlinearities than standard nonlinear materials [2], they failed to bring such systems fully in the quantum regime [11]. For example, in the recently observed polariton blockade, a consequence of the polaritonic interactions at the two-particle level [12,13], only a weak violation of the classical regime has been observed, due to the low interaction over dissipation ratio. These results have strongly motivated the quest for the enhancement of the nonlinearities in polariton based systems.

Recently, evidence has been given that increasing the lengths of aligned exciton dipoles brings an enhancement of the polaritonic interactions in both vertical microcavities [14], and waveguides (WGs) [15,16], due to dipolar long range interactions between excitons. This very promising phenomenon could be exploited for many nonlinear optical effects or for the design of logic gates working at the two-particle regime [17]. However, up to now, direct evidence that dipolar nonlinearities can actually truly work to enhance polariton interaction, for instance via resonant nonlinear parametric effects, is still missing, with only indirect, nonresonant proofs that have been provided, as is the overall blueshift of the exciton resonance [14–16] or the polariton condensation threshold [18]. Nevertheless, the overall blueshift is often due to a concurrence of different factors such as phase space filling, charge screening, reduction of the Rabi coupling, and presence of dark excitonic states which can lead to puzzling results. The WG geometry, a system in which the photonic mode is confined into a 2D slab by total internal reflection [15,19], seems particularly promising for the study and development of optoelectronic devices [20], thanks to features such as faster propagating particles, a geometry that favors the integration of polaritonic optical circuits, high quality factors of the photonic mode, and less demanding growth requirements. Most importantly, the WG platform allows the application of an external electric field perpendicular to the propagation direction able to control

 

the polariton-polariton interaction strength through the manipulation of the exciton dipole length [16,21].

In this Letter, we demonstrate that dipolar polariton-polariton interactions do enhance parametric effects well beyond those derived by standard particle-particle exchange interactions. This is done by measuring the self phase modulation (SPM) of a resonant pulsed wave packet propagating in the same kind of sample studied in [15,16,21]. Moreover, we use this effect to make a precise and unequivocal assessment of the strength of the polariton dipolar interaction. A short pulse propagating inside a polariton WG undergoes a parametric effect [2] known as SPM. SPM is a well-known third order nonlinear effect [22] seen in optical systems as caused by the modification of the refractive index due to the propagation of the pulse itself and resulting in a spectral broadening and, for higher powers, structuring of the propagating pulse. However, the same effect can be seen, for strongly interacting particles, as a spontaneous parametric scattering, a four wave mixing process, that leads to depletion of the packet at the highest density point, in favor of a spread of particles along the propagation dispersion. Here, we measure the SPM-induced pulse spectral modification in an AlGaAs/GaAs WG-QW system, directly showing the enhancement of the parametric effect by dipolar polariton-polariton interactions, introduced by means of a perpendicular electric field. The measured data are accurately fitted by a Gross-Pitaevskii (GP) model allowing extracting the real dipolar enhancement of polariton-polariton interactions. Remarkably, we measure onto the parametric effect a fivefold enhancement of excitonic interactions due to the change in the dipole length.

The WG structure is grown on an $n^+$-doped GaAs substrate, on top of which a 500 nm cladding of $Al_{0.8}Ga_{0.2}As$ was previously deposited. The structure consists of 12 pairs of 20 nm thick GaAs QWs separated by 20 nm of $Al_{0.4}Ga_{0.6}As$ barriers [15,16], resulting in a photonic mode with a quality factor of $\sim 10^4$. We process the slab WG through a dry etching technique [23] in order to fabricate a 1 $\mu$m wide, 200 $\mu$m long wire, confining polaritons in one additional direction and further reducing the modal volume. With this technique, we also fabricate focusing gratings [24] or tapers to efficiently inject and extract the laser pulse into the small-volume waveguide. A schematic model of the WG system, comprising the input or output tapered gratings, is displayed in Fig. 1(a). Finally, the slab surface is covered with a 50 nm layer of indium tin oxide (ITO), that, together with the doped substrate on the opposite side, enables the appliance of an external electric field in the direction perpendicular to the slab plane [16] [see Supplemental Material (SM) [25] for additional details on sample etching and processing]. Figure 1(b) shows the energy dispersion of the zero-order polaritonic modes in absence of external fields.

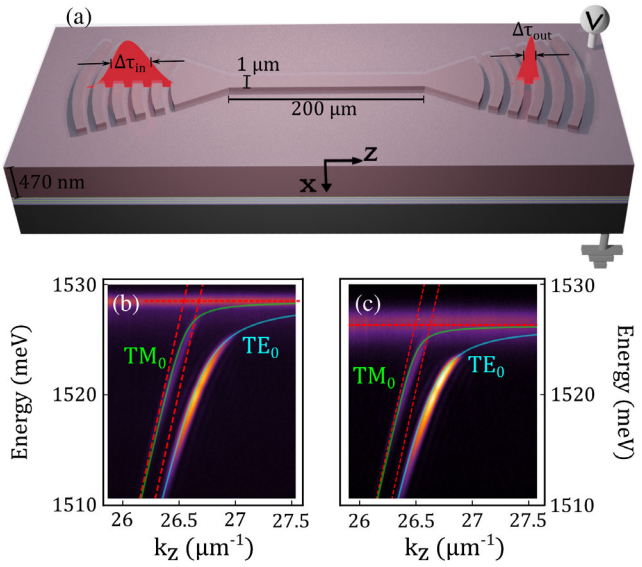


FIG. 1. (a) A slab waveguide is patterned through an etching process to create a wire 1 $\mu$m wide with input and output focusing gratings. The incident laser pulse resonantly injects population into the system, and the output signal, modified by the nonlinearities resulting from polaritonic interactions, is collected and analyzed. The doped substrate, together with the ITO capping layer, enables the application of an electric field along the growth direction. (b) Angle and energy-resolved PL emission showing polariton dispersion in the WG system without applied electric field. (c) As in (b), for an applied electric field $E = 11.9$ kV/cm, resulting in the Stark shift of the excitonic energy. Continuous lines in (b) and (c) are calculated polariton dispersion.

As reported in previous works [15,26], the geometry and polarization of the guided electromagnetic modes yield a Rabi splitting around 3 times higher for the transverse electric (TE) than for the transverse magnetic (TM) mode. The value of the Rabi splitting is $\Omega = 13.9$ meV for the TE mode and $\Omega = 5.8$ meV for the TM mode. Because of the greater exciton-TE mode coupling, all the measurements are performed on this mode. When an electric field is applied to the structure [15], the spatial profile of the potential energy of the QW is modified. The induced spatial separation between electrons and holes results in a finite dipole in a photocreated electron-hole pair [27,28]. As a consequence, the exciton energy shifts and the Rabi splitting slightly diminishes, as is shown in Fig. S2 in the (SM) [25]. The range of fields explored in this Letter corresponds to the regime characterized by a quadratic Stark energy shift [27], in which exciton dissociation due to the applied field can be neglected. By using a variational approach [28], we extract an induced dipole length around 4 nm for Fig. 1(c) in agreement with previous works [14–16]. The laser pulse is focused on the input taper, that injects the light into the $TE_0$ mode of the microwire. After propagating along its 200 $\mu$m, it is extracted by a second taper, see sketch in Fig. 1(a). The light is then collected and analyzed by a spectrometer, see

SM [25] for further details. During the pulse propagation, the time-dependent pulse intensity modifies the refractive index of the medium, due to $\chi^{(3)}$ nonlinearities provided by polariton-polariton interactions, resulting in the SPM effect. Figure 1(a) shows that the time-dependent modification of the refractive index can be intuitively understood as an induced temporal compression of the propagating pulse and, hence, the observed SPM spectral broadening. This effect can also be viewed as a particle-particle scattering mechanism: two particles injected with the same energy and wave vector can interact and scatter toward two different states fulfilling the energy and momentum conservation conditions [2,22].

Figures 2(a) and 2(b) show 2D representations of the pulse spectra obtained after resonant nonlinear propagation through the WG. The $x$ axis represents the calculated exciton density, which is proportional to the excitation power (see description of the theoretical model below and a discussion of the relationship between input power and exciton density in the SM [25]). We note that the absolute value of $g$ and, thus, the absolute value of the density, are not measured in this experiment, and instead, we observe their scaling as a function of input power. Figure 2(a) shows the propagation without applied electric field and Fig. 2(b) the propagation for $E = 11.9$ kV/cm. In both cases, the laser energy is tuned to be at excitonic fraction $X^2 = 0.5$. Both figures show a density-dependent spectral broadening and structuring of the propagating pulse [2,22]. Remarkably, the pulse broadening in the presence of an applied field in Fig. 2(b) is larger and occurs at lower exciton densities than in the case without an applied electric field in Fig. 2(a). Moreover, in the presence of the applied electric field, the output pulse shows a more pronounced structure. At higher excitation powers, the high-intensity part (the central peak) of the propagating pulse is depleted by the particle-particle scattering resulting in a more complex structure of the output pulse [22]. This is a signature of the nonlinear pulse propagation and can be understood in terms of a peak depletion due to the particle-particle scattering. Figure 2 also shows an asymmetric broadening, with the red part of the propagating pulse being more intense than the blue part. This is due to both the shape of the polariton dispersion and the increased absorption on the blue side due to the excitonic tail. We note that, for $E = 11.9$ kV/cm, the output intensities are roughly half the output intensities without any applied electric field. We assign this discrepancy to a slight increase of nonradiative losses in the presence of the electric field (see, also, discussion below). Figures 2(c)–2(e) show spectra of the output pulse at zero field (red lines) and at $E = 11.9$ kV/cm (green lines) at exciton densities equal to 1, 7, and 19 excitons per $\mu$m$^2$, see corresponding vertical dashed lines in Figs. 2(a) and 2(b). These figures show that, at low exciton density, see Fig. 2(c), the nonlinearity does not affect the pulse shape, and the two spectra have identical linewidths. When the exciton density is increased, Fig. 2(d), the applied electric field causes a larger broadening of the output pulse. At even higher exciton densities, Fig. 2(e), the pulse propagating under the action of the applied electric field shows a pronounced structure with the presence of two lobes, while the pulse propagating without an applied electric field keeps a single peak shape.

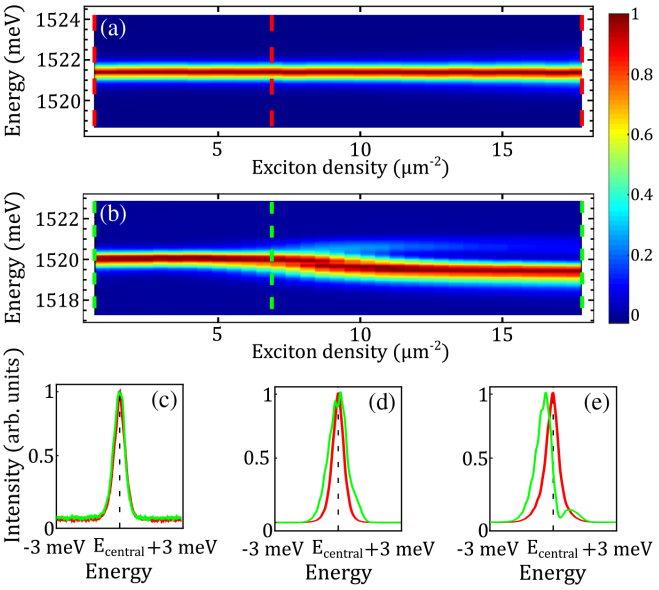


FIG. 2. (a) Normalized output pulse spectra as a function of the exciton densities. (b) Same as panel (a) but for an applied transverse electric field of 11.9 kV/cm; nonlinear effects in (b) are visible at exciton densities lower than in (a), a signature of the dipolar enhancement of polariton-polariton interactions. (c)–(e) Pulse broadening and structuring for three different exciton densities indicated by vertical lines on the 2D maps of panels (a) and (b); the red spectra correspond to the case in which no electric field acts on the system, while green spectra correspond to an electric field value of 11.9 kV/cm; spectra are energy shifted to compare shape and FWHM.

The effect of the electric field on the SPM-induced broadening is also clearly visible in Fig. 3, showing the FWHM of the output pulse as a function of the exciton densities for different applied electric fields (keeping the same excitonic fraction $X^2 = 0.5$ for each field). Filled points refer to the range of exciton densities in which the output pulse shows a single broadened peak. Empty circles refer to the range of exciton densities in which the output pulse shows a structured peak (in this case, each point represents the FWHM of the more intense lobe). As the applied electric field increases, the pulse broadening at a given polariton density increases, showing a clear dipolar enhancement of the parametric effects. Moreover, pulse breaking, i.e., the transition from filled points to empty circles, takes place at lower excitonic density when the applied electric field is increased, highlighting the dipolar enhancement of polariton-polariton scattering.

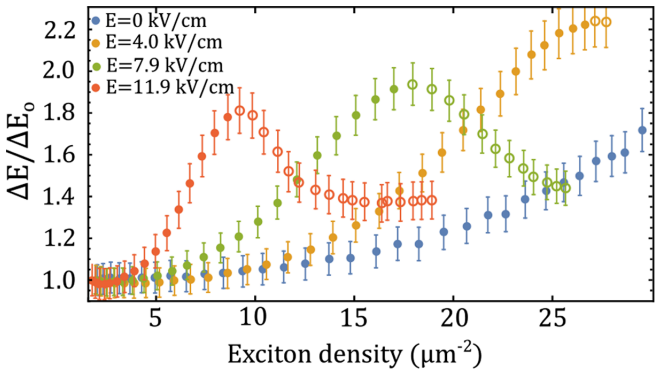


FIG. 3. FWHM of the spectra from a Gaussian fit as a function of the output power for four different values of the electric field. The output pulse width is normalized to the incident width. The empty circles correspond to the cases in which the output spectrum has several peaks and represent the linewidths of the most intense lobe.

To obtain a quantitative description of the observed dipolar enhancement of the polariton-polariton interactions, we solve the coupled equations [2] 1(a) and 1(b) describing the system dynamics in the GP formalism

$$\left[i\frac{\partial}{\partial t}+i\gamma_p+\nu_g\left(i\frac{\partial}{\partial z}+\frac{1}{2k_z}\frac{\partial^2}{\partial x^2}\right)\right]A=\left(\frac{\Omega}{2}\right)\Psi, \quad (1a)$$

$$\left[i\frac{\partial}{\partial t}+i\gamma_e-g|\Psi|^2\right]\Psi=\left(\frac{\Omega}{2}\right)A, \quad (1b)$$

where $A$ and $\Psi$ are the photon and exciton wave-function amplitudes, respectively. $\nu_g$ is the photon group velocity obtained from the theoretically fitted dispersion, and $k_z$ the corresponding linear momentum. $\gamma_p$ and $\gamma_e$ are the decay rates of the coherent photonic and excitonic states. The evolution of the initial (∼2 ps or ∼145 $\mu$eV) pulse is calculated by solving Eqs. (1) obtaining a theoretical output spectrum for each input power. A nonlinear least square routine is used to determine $g$, as well as the detuning and duration of the pump pulse, minimizing the difference between the measured and simulated matrices of power vs spectrum. Figure 4 shows the measured (left column) and calculated (right column) spectra as function of the input power for each of the four applied electric fields, with an excellent agreement between experimental data and simulations. It is worth noting that, here, we are focusing on the dipolar enhancement of polariton-polariton interactions. In particular, we have fixed the value of $g = 6\ \mu\text{eV}\,\mu\text{m}^2$ at zero applied electric field [29] and found the corresponding exciton density per QW. Based on the obtained exciton density and on the measured output intensities, it is possible to retrieve the exciton density or output intensity calibration. We calibrate based on the peak value of $|\Psi|^2$ observed at the end of the waveguide in the simulation. Then, we

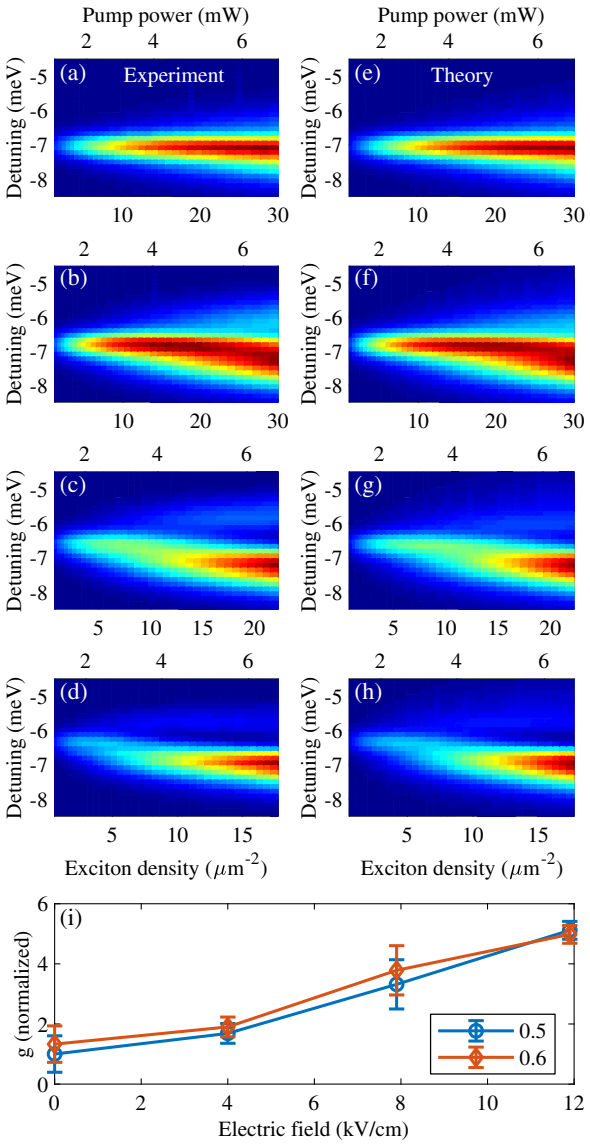


FIG. 4. (a)–(d) Measured density maps of the output spectra as a function of estimated exciton density at the end of the waveguide for field strengths of 0, 4, 7.9, and 11.9 kV/cm, respectively, and placed on a constantly spaced photon energy grid for comparison to simulations, for an excitonic fraction of 0.5. (e)–(h) Corresponding results of numerical solution of the Gross-Pitaevskii equation for guided exciton polaritons after nonlinear least squares fitting to determine the value of the interaction constant $g$. See the text for the calibration of the $|\Psi|^2$ axis. (i) Electric field dependence of the fitted value of the parameter $g$, for two different excitonic fractions, 0.5 and 0.6, normalized to the value at zero field and fraction of 0.5.

have used this calibration to determine the exciton densities for the entire data set (see SM [25] and, in particular, Fig. S4 for the details). Figure 4(i) shows that the enhancement of the dipolar interaction with the field causes $g$ to increase by a factor ≈5 under the strongest electric field applied in the experiment. To show the consistency of our approach, we have reported values of $g$ obtained on two

different sets of data measured at excitonic fractions $X^2 = 0.5$ and $X^2 = 0.6$.

Remarkably, while we find a significant enhancement of polariton-polariton interactions due to the applied electric field, this enhancement is at least an order of magnitude smaller than the one reported on a sample having the same design [16] by measuring nonresonant blueshift of the polariton resonance. We believe, as mentioned above, that this discrepancy is essentially due to the fact that the polariton blueshift is only an indirect measurement of the particle-particle interaction that could be caused by many different effects. As a matter of fact, we have also performed nonresonant experiments under ultrafast pumping, observing a wide range of possible blueshifts at a given excitation power. The cause of such behavior is due to multiple factors not all related to the dipole enhancement and possibly dependent on extrinsic parameters. Nonresonant excitation could be responsible for the creation of trapped electric carriers that, under the action of the applied electric field and depending on the quality of the electric contacts, can induce a screening phenomenon. Such a screening may reduce the Stark effect and result in an apparent blueshift. In contrast, in this Letter we measure polariton-polariton interactions through a different effect, the SPM, which cannot be enhanced by other effects including screening. We also stress that the use of an ultrafast picosecond exciting pulse is important to reduce other spurious causes, such as the creation of a long living, "dark" exciton reservoir [29], that contribute to the overall density without being detected. Particularly, in the WG platform, the presence of a long-lived excitonic reservoir can alter the measurement of the interaction strength by more than 2 orders of magnitude [30,31]. To avoid these possible spurious effects, we resonantly inject the population with a pulsed laser of 80 MHz repetition rate and $\sim$2 ps ($\sim$145 $\mu$eV) pulse duration (spectral width). Our results are in qualitative agreement with the enhancement reported under resonant reflectivity in the case of permanent electric dipoles stemming from indirect excitons in double QWs [14].

In conclusion, we demonstrated that parametric effects in polaritonic systems can be enhanced by polarizing their excitonic component thanks to an applied electric field. By measuring the self-phase modulation of a propagating waveguide packet, we find a fivefold enhancement of polariton-polariton interactions. However, in the case of systems with very weak nonlinearities, such a dipolar effect, which is independent of the intrinsic polariton exchange interaction, could even lead to enhancements an order of magnitude higher. For instance, we believe that this enhancement method could be extremely effective in transition metal dichalcogenides-based polariton systems. These results are essential to assess the relevance of dipolar polariton waveguides for future integrated and quantum optics application [32,33] and to guide the development of a new generation of WG polaritons supporting stronger nonlinearities, even at room temperature.

We thank Paolo Cazzato for technical support. We are grateful to Ronen Rapaport for inspiring discussions and for sharing information about the sample design. The authors acknowledge the project PRIN Interacting Photons in Polariton Circuits INPhoPOL [Ministry of University and Scientific Research (MIUR), Grant No. 2017P9FJBS_001]. Work at the Molecular Foundry was supported by the Office of Science, Office of Basic Energy Sciences, of the U.S. Department of Energy under Contract No. DE-AC02-05CH11231. We thank Scott Dhuey at the Molecular Foundry for assistance with the electron beam lithography. We acknowledge the project FISR—C. N. R. Tecnopolo di nanotecnologia e fotonica per la medicina di precisione—CUP B83B17000010001 and "Progetto Tecnopolo per la Medicina di precisione, Deliberazione della Giunta Regionale Grant No. 2117. This research is funded in part by the Gordon and Betty Moore Foundations EPiQS Initiative, Grant No. GBMF9615 to L. N. Pfeiffer, and by the National Science Foundation MRSEC Grant No. DMR 1420541.

*vincenzo.ardizzone@nanotec.cnr.it
†nicholas.karpowicz@nanotec.cnr.it

[1] D. Ballarini, M. De Giorgi, E. Cancellieri, R. Houdré, E. Giacobino, R. Cingolani, A. Bramati, G. Gigli, and D. Sanvitto, All-optical polariton transistor, Nat. Commun. **4** (2013).
[2] P. M. Walker, C. E. Whittaker, D. V. Skryabin, E. Cancellieri, B. Royall, M. Sich, I. Farrer, D. A. Ritchie, M. S. Skolnick, and D. N. Krizhanovskii, Spatiotemporal continuum generation in polariton waveguides, Light Sci. Appl. **8**, 6 (2019).
[3] S. Slussarenko and G. J. Pryde, Photonic quantum information processing: A concise review, Appl. Phys. Rev. **6**, 041303 (2019).
[4] F. Flamini, N. Spagnolo, and F. Sciarrino, Photonic quantum information processing: A review, Rep. Prog. Phys. **82**, 016001 (2019).
[5] J. J. Baumberg, P. G. Savvidis, R. M. Stevenson, A. I. Tartakovskii, M. S. Skolnick, D. M. Whittaker, and J. S. Roberts, Parametric oscillation in a vertical microcavity: A polariton condensate or micro-optical parametric oscillation, Phys. Rev. B **62**, R16247 (2000).
[6] A. Baas, J. Ph Karr, M. Romanelli, A. Bramati, and E. Giacobino, Optical bistability in semiconductor microcavities in the nondegenerate parametric oscillation regime: Analogy with the optical parametric oscillator, Phys. Rev. B **70**, 161307 (2004).
[7] A. Amo, J. Lefrère, S. Pigeon, C. Adrados, C. Ciuti, I. Carusotto, R. Houdré, E. Giacobino, and A. Bramati, Superfluidity of polaritons in semiconductor microcavities, Nat. Phys. **5**, 805 (2009).
[8] G. Lerario, A. Fieramosca, F. Barachati, D. Ballarini, K. S. Daskalakis, L. Dominici, M. De Giorgi, S. A. Maier, G. Gigli, S. Kéna-Cohen, and D. Sanvitto, Room-temperature superfluidity in a polariton condensate, Nat. Phys. **13**, 837 (2017).

[9] V. Ardizzone, P. Lewandowski, M. H. Luk, Y. C. Tse, N. H. Kwong, A. Lcke, M. Abbarchi, E. Baudin, E. Galopin, J. Bloch, A. Lemaitre, P. T. Leung, P. Roussignol, R. Binder, J. Tignon, and S. Schumacher, Formation and control of turing patterns in a coherent quantum fluid, Sci. Rep. **3** (2013).

[10] K. G. Lagoudakis, M. Wouters, M. Richard, A. Baas, I. Carusotto, R. André, L. S. Dang, and B. Deveaud-Plédran, Quantized vortices in an excitonpolariton condensate, Nat. Phys. **4**, 706 (2008).

[11] D. Sanvitto and S. Kéna-Cohen, The road towards polaritonic devices, Nat. Mater. **15**, 1061 (2016).

[12] G. Muñoz-Matutano, A. Wood, M. Johnsson, X. Vidal, B. Q. Baragiola, A. Reinhard, A. Lemaître, J. Bloch, A. Amo, G. Nogues, B. Besga, M. Richard, and T. Volz, Emergence of quantum correlations from interacting fibre-cavity polaritons, Nat. Mater. **18**, 213 (2019).

[13] A. Delteil, T. Fink, A. Schade, S. Höfling, C. Schneider, and A. mamolu, Towards polariton blockade of confined excitonpolaritons, Nat. Mater. **18**, 219 (2019).

[14] E. Togan, H. T. Lim, S. Faelt, W. Wegscheider, and A. Imamoglu, Enhanced Interactions between Dipolar Polaritons, Phys. Rev. Lett. **121**, 227402 (2018).

[15] I. Rosenberg, Y. Mazuz-Harpaz, R. Rapaport, K. West, and L. Pfeiffer, Electrically controlled mutual interactions of flying waveguide dipolaritons, Phys. Rev. B **93**, 195151 (2016).

[16] I. Rosenberg, D. Liran, Y. Mazuz-Harpaz, K. West, L. Pfeiffer, and R. Rapaport, Strongly interacting dipolar-polaritons, Sci. Adv. **4** (2018).

[17] M. Heuck, K. Jacobs, and D. R. Englund, Controlled-Phase Gate Using Dynamically Coupled Cavities and Optical Nonlinearities, Phys. Rev. Lett. **124** (2020).

[18] S. I. Tsintzos, A. Tzimis, G. Stavrinidis, A. Trifonov, Z. Hatzopoulos, J. J. Baumberg, H. Ohadi, and P. G. Savvidis, Electrical Tuning of Nonlinearities in Exciton-Polariton Condensates, Phys. Rev. Lett. **121**, 037401 (2018).

[19] P. M. Walker, L. Tinkler, M. Durska, D. M. Whittaker, I. J. Luxmoore, B. Royall, D. N. Krizhanovskii, M. S. Skolnick, I. Farrer, and D. A. Ritchie, Exciton polaritons in semiconductor waveguides, Appl. Phys. Lett. **102**, 012109 (2013).

[20] D. G. Suárez-Forero, F. Riminucci, V. Ardizzone, M. de Giorgi, L. Dominici, F. Todisco, G. Lerario, L. N. Pfeiffer, G. Gigli, D. Ballarini, and D. Sanvitto, Electrically controlled waveguide polariton laser, arXiv:2003.02198v2.

[21] D. Liran, I. Rosenberg, K. West, L. Pfeiffer, and R. Rapaport, Fully guided electrically controlled exciton polaritons, ACS Photonics **5**, 4249 (2018).

[22] G. Agrawal, *Nonlinear Fiber Optics* (Academic Press, New York, 2003).

[23] Z. Liao and J. Stewart Aitchison, Precision etching for multi-level AlGaAs waveguides, Opt. Mater. Express **7**, 895 (2017).

[24] K. K. Mehta and R. J. Ram, Precise and diffraction-limited waveguide-to-free-space focusing gratings, Sci. Rep. **7**, 1 (2017).

[25] See Supplemental Material at http://link.aps.org/supplemental/10.1103/PhysRevLett.126.137401 for description of the theoretical model and of the fitting procedure.

[26] P. Yu. Shapochkin, M. S. Lozhkin, I. A. Solovev, O. A. Lozhkina, Y. P. Efimov, S. A. Eliseev, V. A. Lovcjus, G. G. Kozlov, A. A. Pervishko, D. N. Krizhanovskii, P. M. Walker, I. A. Shelykh, M. S. Skolnick, and Y. V. Kapitonov, Polarization-resolved strong lightmatter coupling in planar GaAs/AlGaAs waveguides, Opt. Lett. **43**, 4526 (2018).

[27] G. Bastard, *Wavemechanics Applied to Semiconductor Heterostrutures* (EDP Sciences, Les Ulis, France, 1988).

[28] G. Bastard, E. E. Mendez, L. L. Chang, and L. Esaki, Variational calculations on a quantum well in an electric field, Phys. Rev. B **28**, 3241 (1983).

[29] E. Estrecho, T. Gao, N. Bobrovska, D. Comber-Todd, M. D. Fraser, M. Steger, K. West, L. N. Pfeiffer, J. Levinsen, M. M. Parish, T. C. H. Liew, M. Matuszewski, D. W. Snoke, A. G. Truscott, and E. A. Ostrovskaya, Direct measurement of polariton-polariton interaction strength in the Thomas-Fermi regime of exciton-polariton condensation, Phys. Rev. B **100**, 035306 (2019).

[30] P. M. Walker, L. Tinkler, D. V. Skryabin, A. Yulin, B. Royall, I. Farrer, D. A. Ritchie, M. S. Skolnick, and D. N. Krizhanovskii, Ultra-low-power hybrid light-matter solitons, Nat. Commun. **6**, 8317 (2015).

[31] P. M. Walker, L. Tinkler, B. Royall, D. V. Skryabin, I. Farrer, D. A. Ritchie, M. S. Skolnick, and D. N. Krizhanovskii, Dark Solitons in High Velocity Waveguide Polariton Fluids, Phys. Rev. Lett. **119**, 097403 (2017).

[32] D. G. Suárez-Forero, V. Ardizzone, S. F. Covre da Silva, M. Reindl, A. Fieramosca, L. Polimeno, M. de Giorgi, L. Dominici, L. N. Pfeiffer, G. Gigli, D. Ballarini, F. Laussy, A. Rastelli, and D. Sanvitto, Quantum hydrodynamics of a single particle, Light Sci. Appl. **9**, 85 (2019).

[33] Á. Cuevas, J. C. López Carreño, B. Silva, M. De Giorgi, D. G. Suárez-Forero, C. Sánchez Muñoz, A. Fieramosca, F. Cardano, L. Marrucci, V. Tasco, G. Biasiol, E. Del Valle, L. Dominici, D. Ballarini, G. Gigli, P. Mataloni, F. P. Laussy, F. Sciarrino, and D. Sanvitto, First observation of the quantized exciton-polariton field and effect of interactions on a single polariton, Sci. Adv. **4** (2018).